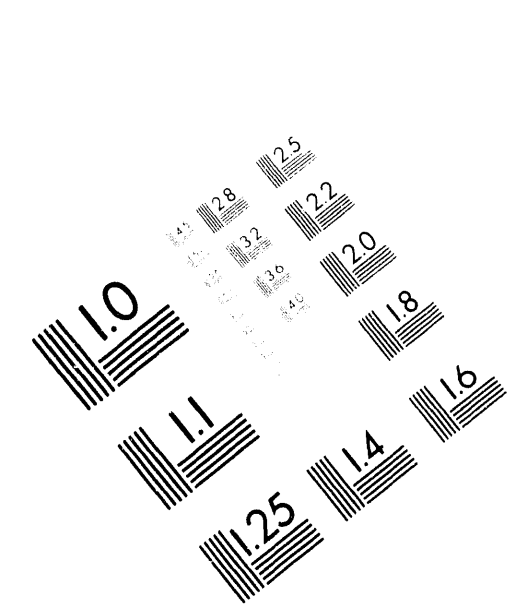

AIIM

Association for Information and Image Management

1100 Wayne Avenue, Suite 1100
Silver Spring, Maryland 20910

301/587-8202

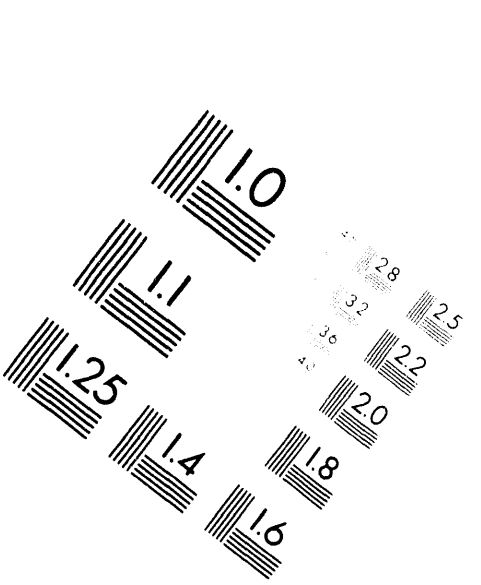

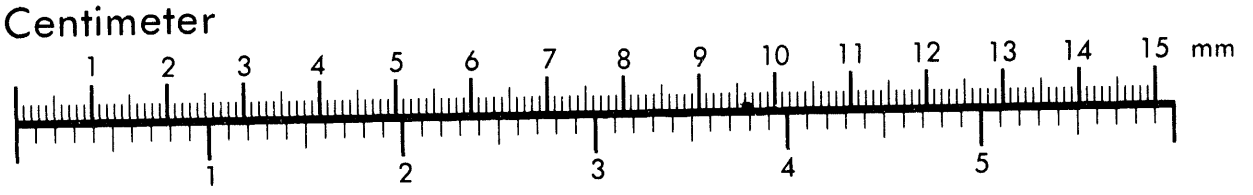

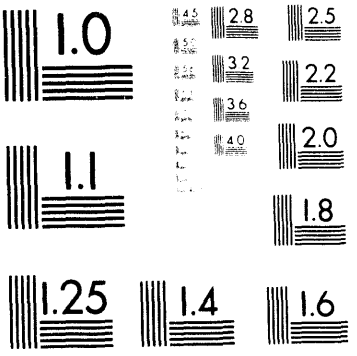

MANUFACTURED TO AIIM STANDARDS
BY APPLIED IMAGE, INC.

1 of 1

Conf-941075--1

LA-UR-94- 2891
TSA-11-94-R104

Los Alamos National Laboratory is operated by the University of California for the United States Department of Energy under contract W-7405-ENG-36

TITLE: SIMULTANEOUS TRANSPORT OF SYNTHETIC COLLOIDS AND A NONSORBING SOLUTE THROUGH SINGLE SATURATED NATURAL FRACTURES

AUTHOR(S): P. W. Reimus
B. A. Robinson
H. E. Nuttall
R. Kale

SUBMITTED TO: Scientific Basis for Nuclear Waste Management XVIII
October 23-27, 1994
Kyoto, Japan

Los Alamos
Los Alamos National Laboratory
Los Alamos, New Mexico 87545

SIMULTANEOUS TRANSPORT OF SYNTHETIC COLLOIDS AND A NONSORBING SOLUTE THROUGH SINGLE SATURATED NATURAL FRACTURES

PAUL W. REIMUS,* B. A. ROBINSON,* H. E. NUTTALL,** AND R. KALE**
*Los Alamos National Laboratory, Los Alamos, NM 87545
**University of New Mexico, Albuquerque, NM 87131

ABSTRACT

Tracer transport experiments involving colloids that showed little tendency to attach to rock surfaces and a nonsorbing solute (iodide) were conducted in three different well-characterized natural fractures in tuff. The colloids always arrived earlier in the effluent than the iodide, which we believe is evidence of (1) hydrodynamic chromatography and/or (2) the fact that the colloids experience a smaller effective volume in the fracture because they diffuse too slowly to enter low-velocity regions (dead zones) along the rough fracture walls. The iodide also approached the inlet concentration in the effluent more slowly than the colloids, with the concentration at a given elution volume being greater at higher flow rates. By contrast, the rate of approach of the colloid concentration to the inlet concentration did not vary with flow rate. We attribute this behavior to matrix diffusion of the iodide, with the colloids being too large/nondiffusive to experience this phenomenon. Dispersion of all tracers was greatest in the fracture of widest average aperture and least in the fracture of narrowest aperture, which is consistent with Taylor dispersion theory.

The tracer experiments were modeled/interpreted using a three-step approach that involved (1) estimating the aperture distribution in each fracture using surface profiling techniques, (2) predicting the flow field in the fractures using a localized parallel-plate approximation, and (3) predicting tracer transport in the fractures using particle-tracking techniques. Although considered preliminary at this time, the model results were in qualitative agreement with the experiments.

BACKGROUND

Colloids have the potential to move through saturated groundwater systems faster than nonsorbing solutes because their large size and low diffusivity tend to exclude them from regions of low groundwater velocity.[1,2] In fractured media, groundwater flow is limited almost exclusively to fractures, but diffusion into pores in the rock matrix (known as "matrix diffusion") can significantly retard the transport of solutes relative to that of water.[3,4] By contrast, colloids should be largely excluded from the rock matrix and could possibly move through a fractured system more rapidly than the average water velocity because of their tendency as slowly diffusing species to remain in high-velocity fluid streamlines. Whether or not colloids actually experience enhanced mobility in such systems will depend on the nature of the colloid-matrix interactions, with unfavorable deposition interactions (i.e., the tendency for colloids to <u>not</u> deposit on rock surfaces) resulting in enhanced mobility.

The possibility of rapid colloid transport poses significant challenges for performance assessments of geologic waste disposal sites such as high-level nuclear waste repositories. However, it also suggests an opportunity to conduct more thorough tracer transport studies to characterize geohydrologic systems. Hydrodynamic dispersion and chemical retardation in such systems have often been studied by doing tracer experiments with a suite of solutes that have different diffusivities and/or different reactivities with the geologic media.[4] The breakthrough curves of nonreacting solutes are frequently used to infer the true hydrodynamic dispersion in a system. In saturated fractured media, the observed dispersion may be dominated by matrix diffusion. If colloids are excluded from the porous matrix because of size/diffusivity considerations and if they have unfavorable deposition interactions with the matrix, they could, in principle, be used as tracers in conjunction with solutes to provide a means of estimating how much of the observed solute dispersion is due to matrix diffusion. This information could help provide a defensible basis for (1) taking credit for matrix diffusion as a mechanism of solute

retardation/attenuation in performance assessments, and (2) predicting colloid transport and dispersion in fractured media under worst-case conditions of minimal deposition. These two possibilities inspired the work described in this paper.

EXPERIMENTAL

Materials and Methods

Tracer experiments were conducted in three natural fractures: (1) Bandelier tuff from an outcropping near Los Alamos, New Mexico (11.3- x 10.1-cm surface area, ~0.6-cm^3 void volume/~55-μm average aperture, ~30-μm hydraulic aperture, and 0.089 matrix porosity), (2) Tram tuff from a Nevada Test Site core sample (9.7- x 8.4-cm surface area, ~1.3-cm^3 void volume/~160-μm average aperture, ~90-μm hydraulic aperture, and 0.192 matrix porosity), and (3) Bullfrog tuff from a Nevada Test Site core sample (8.5- x 8.3-cm surface area, ~3.7-cm^3 void volume/~555-μm average aperture, ~110-μm hydraulic aperture, and 0.208 matrix porosity). The void volumes and hydraulic apertures were estimated from tracer residence times and flow resistances, respectively. Porosities were measured by weight difference of saturated and unsaturated tuff blocks of known volume (done in triplicate).

Each fracture bisected a roughly rectangular block that had been cut to allow construction of a leak-free flow system around the fracture. The fracture surfaces were joined under moderate pressure using aluminum confining plates bolted together at the corners. No-flow boundaries were imposed on two sides of the fracture by compressing silicone gasket material over the rock under an aluminum plate. Constant pressure boundaries were imposed on the ends using the same technique but with a channel cut out of the gasket material to serve as a flow manifold. The flow system could be assembled completely under water, thereby assuring that no air bubbles were entrapped in the fracture, and it could be easily and quickly disassembled after tracer experiments to examine the fracture surfaces for deposited colloids.

Tracers used in the experiments included:

1. 1-μm-diam carboxylate-modified polystyrene latex (CML) microspheres,
2. 0.3-μm-diam CML microspheres, and
3. lithium iodide (iodide serving as a nonsorbing solute).

The polystyrene latex colloids (from Interfacial Dynamics Corp., Portland, OR) were tagged with fluorescent dyes, which allowed discrimination and concentration measurement using flow cytometry. Iodide was analyzed using an ion-selective electrode. Earlier work[5] had established that the CML microspheres moved through the fractures with less deposition than either non-CML polystyrene or silica microspheres. The colloids and tuff surfaces all had significant negative surface charges (as determined by zeta potential measurements).

All three tracers were introduced simultaneously in each experiment to ensure that they all experienced the same flow conditions. The tracers were introduced as a uniform step by flushing the inlet manifold with the tracer solution before allowing flow through the fracture. Flow rates through the fracture were controlled using a peristaltic pump. In all tests, the outlet manifold was continuously flushed with tracer-free solution to reduce the tracer residence time in the manifold and exit tubing. This flushing procedure resulted in a 50- to 600-fold dilution of the solution exiting the fracture (depending on the flow rates), but it ensured that the observed tracer breakthrough curves could be attributed entirely to dispersion and interactions within the rock, not within the tubing or manifold.

Temperatures in all experiments were ambient, ranging from 21 to 26°C. The tracer-free solution was silica-saturated, sodium/calcium bicarbonate well water taken from well J-13 at the Nevada Test Site; the solution had an approximate ionic strength of 0.003 M. The water was filtered with a 0.2-μm cartridge filter before being used in the experiments. The tuff blocks were saturated under vacuum for several months before the tracer experiments were conducted. Batch sorption experiments were conducted to check for iodide sorption on the tuffs. These tests

indicated no measurable sorption of iodide on any of the samples. Mineralogical characterization of the fractures was pending at the time this paper was prepared.

After the completion of the tracer experiments, an attempt was made to determine the aperture distribution within the fractures by profiling the fracture surfaces and then mathematically manipulating the surface data to estimate apertures as a function of position. The surfaces were profiled using the PEAK profilometer at Lawrence Livermore National Laboratory.[6] The profiles featured a 0.25-mm spacing between data points in the x- and y-directions (in the plane of the fracture) and a standard deviation of approximately 5 μm in the z-direction.

Results

Sixteen tracer experiments were conducted in all, with at least three different flow rates being used in each fracture. The flow rates were chosen to bracket the range expected in forced-gradient field experiments, so they were high relative to natural-gradient conditions (mean tracer residence times varied from approximately 2.5 to 12 min in the fractures). Figure 1 shows typical breakthrough curves for the CML colloids and iodide in the Bandelier tuff fracture. These breakthrough curves are representative of those in all the experiments. The common features in the experiments were as follows.

- The colloids always arrived in the effluent earlier than the iodide and approached the inlet concentration (C_o) more rapidly than iodide. We attribute the earlier colloid arrival to either (1) hydrodynamic chromatography (that is, the iodide more closely follows classical Taylor dispersion in which all the streamlines across the width of the flow channel are sampled and an average fluid velocity is thus experienced, while the colloids tend to remain in fluid streamlines) or (2) the fact that the colloids experience a smaller effective volume in the fracture because they diffuse too slowly to enter low-velocity regions (dead zones) along the rough fracture walls. The difference in arrival time decreased as the average fracture aperture became wider, which is consistent with hydrodynamic chromatography theory. We believe that the slower iodide approach to the inlet concentration was due to matrix diffusion, a phenomenon that did not affect the colloids because they were too large and too slowly diffusing to enter the matrix.

- There was a small but discernable difference between the 1- and 0.3–μm CML colloids in all tests, with the 1-μm colloids arriving slightly earlier than the 0.3-μm colloids. This behavior is consistent with hydrodynamic chromatography theory, which predicts less dispersion (i.e., later arrival) for smaller, more diffusive species.

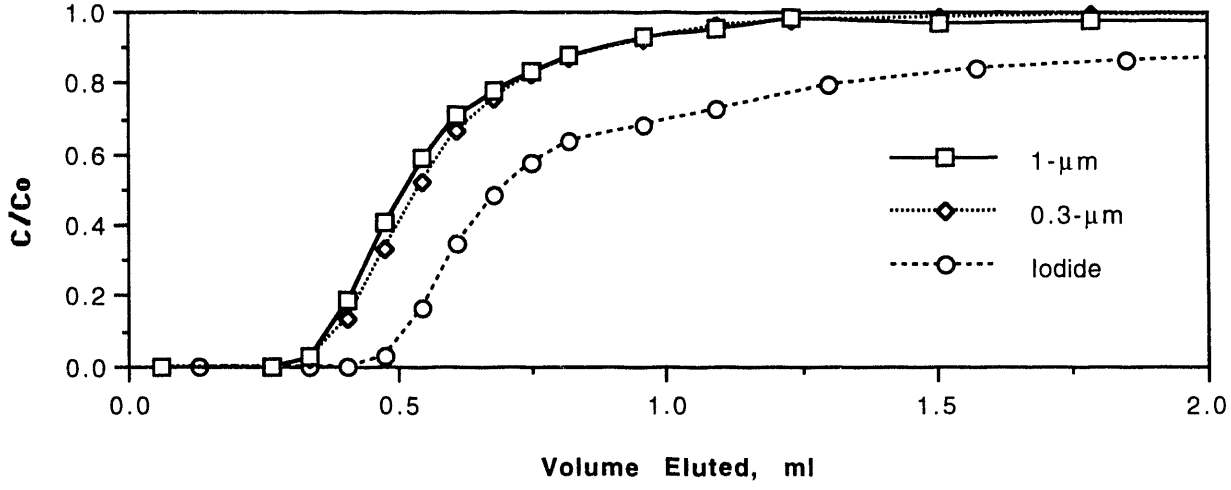

Figure 1. Breakthrough curves of 1-μm and 0.3-μm CML colloids and iodide in the Bandelier tuff fracture. The flow rate was 2.30 μl/sec. Analytical errors are 1-2% for the colloids and 3-5% for the iodide.

- The approach of the iodide concentration to the inlet concentration was dependent on the flow rate in the experiment, with the approach being faster at higher flow rates (when corrected for flow rate differences by plotting on a volume eluted basis). By contrast, the colloid breakthrough curves for a given fracture were identical at all flow rates. These observations are consistent with matrix diffusion as a mechanism that affects iodide but not the colloids. Figure 2 shows iodide breakthrough curves at three different flow rates in the Bandelier tuff fracture.

Another interesting observation during the experiments was that the relative amount of tracer dispersion in the fractures increased as the average fracture aperture increased. This is illustrated in Figure 3, which shows colloid breakthrough curves as a function of void volumes eluted in each of the fractures (void volumes were estimated from the mean residence times of the colloids). The two curves for the Bullfrog tuff fracture correspond to orthogonal flow directions in this fracture. The flow direction was changed by rotating the fracture 90 degrees in the flow system so that the constant pressure boundaries became no-flow boundaries and vice-versa. The Bullfrog fracture was the only fracture for which this was done. It is apparent that dispersion in this fracture was directionally dependent, which suggests the presence of preferential flow pathways that are oriented more strongly in one direction than the other.

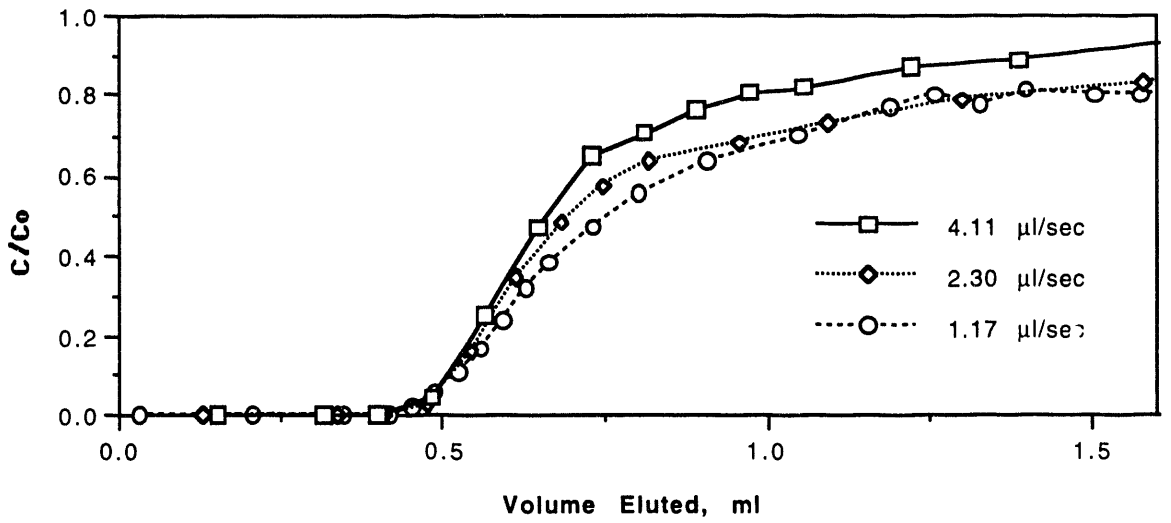

Figure 2. Iodide breakthrough curves in the Bandelier tuff fracture at three different flow rates. Analytical errors are 3-5%.

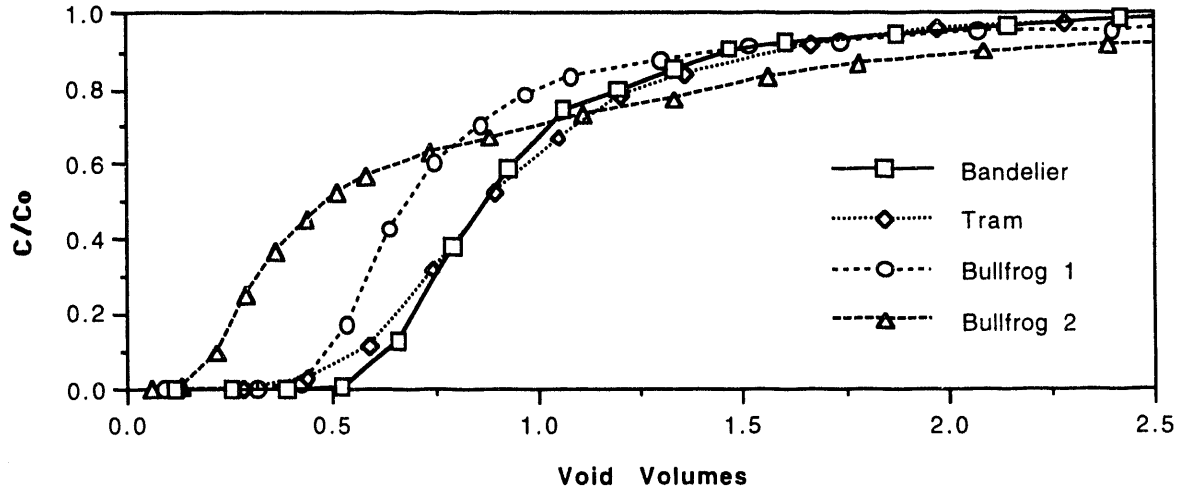

Figure 3. Breakthrough curves of 1-µm CML colloids in each fracture plotted as a function of void volumes eluted. Bullfrog 1 and Bullfrog 2 correspond to orthogonal flow directions in the Bullfrog tuff fracture (see text). Analytical errors are 1-2%.

PREDICTIVE MODELS

After obtaining estimates of the fracture aperture distributions (Figure 1), the steady-state flow field in each fracture was approximated by discretizing the fracture domain into 0.25- x 0.25-mm cells and then solving the continuity equation with the appropriate boundary conditions and assuming that the cubic law for flow between parallel plates applies locally. The details of this approach are described elsewhere.[7,8] The results of these calculations are a pressure distribution within the fracture from which the flow rate across each cell boundary can be calculated. An iterative solution method (implicit alternating direction)[9] was used to estimate the pressure distributions. Nondimensional flow fields within each fracture are depicted in Figure 4.

The nondimensional flow fields were scaled to match the overall flow rates in each of the tracer experiments. Tracer breakthrough curves were then predicted using a particle-tracking technique that made direct use of the calculated flow fields. This approach circumvented the need for an adjustable dispersion parameter because dispersion arose naturally from the meandering flow pathways. The particle tracking calculations were similar to those used by others to predict tracer transport in variable aperture fractures,[8,10] but significant additional logic was necessary to account for hydrodynamic chromatography and matrix diffusion. The details of the approach will be documented in a Ph.D. thesis by one of the authors.[11] Key features include the following.

- Each cell in the computational grid is assumed to have a parabolic velocity profile. The flow distance in each cell is equal to the length of the cell, but a particle can exit across any cell boundary that has outward flow. The particles move through the cells according to:

$$\mathbf{X}^{n+1} = \mathbf{X}^{n} + (\mathbf{v} + \nabla \bullet \mathbf{D})_{\mathbf{X}^n} \Delta t + Z_1 \sqrt{2 D_{\mathbf{X}^n} \Delta t} + Z_2 \sqrt{2 D_{\mathbf{X}^n} \Delta t} \quad , \qquad (1)$$

  where $\mathbf{X}^n, \mathbf{X}^{n+1}$ = particle position at time steps n and n+1,

  $(\mathbf{v} + \nabla \bullet \mathbf{D})_{\mathbf{X}^n}$ = fluid velocity vector plus gradient of diffusivity at position $\mathbf{X}^n$,

  $D_{\mathbf{X}^n}$ = particle diffusivity at position $\mathbf{X}^n$,

  Z_1, Z_2 = independent random numbers with mean of zero and variance of one; the first is used for diffusion in the flow direction and the second is used for diffusion perpendicular to the fracture walls, and

  Δt = time increment.

  However, rather than using explicit time steps, the particles are stepped across the fracture width (perpendicular to cell walls) in distance increments, and a distribution of times is randomly sampled to determine how long it takes to diffuse these distances. The distance moved in the direction of flow during this time is then calculated using the second and third terms on the right-hand side of Equation (1). The particle-to-wall separation distance relative to cell half width is kept constant when a particle moves across cell boundaries.

- When a solute particle "hits" a wall, it has a probability of encountering a pore equal to the matrix porosity. If a pore is not present, the wall is treated as a reflective boundary. When a pore is encountered, a pre-calculated distribution of times is randomly sampled to determine the time it takes for the particle to diffuse a specified distance back into the fracture. This time distribution is generated from a separate particle-tracking calculation in which particles start at the wall and are allowed to diffuse either into or away from the matrix according to a random walk. A gradient of diffusivity and porosity (from values in water to values in the porous matrix) must be incorporated into these calculations to avoid false accumulation of particles within the matrix. This is analagous to the

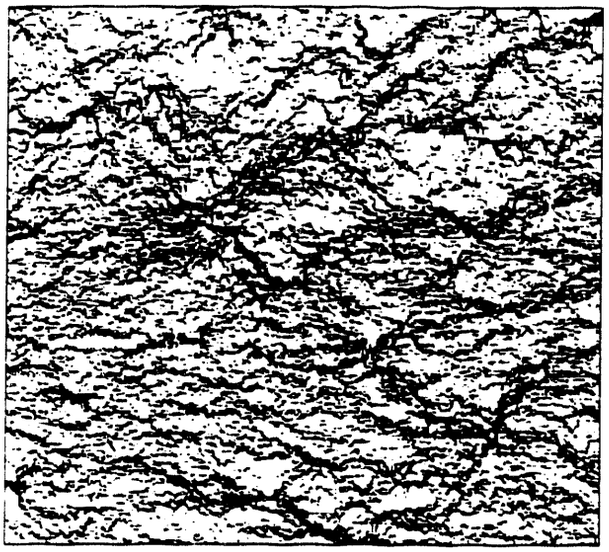

(a)

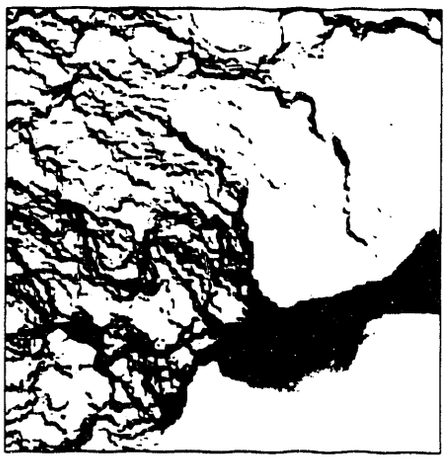

(c)

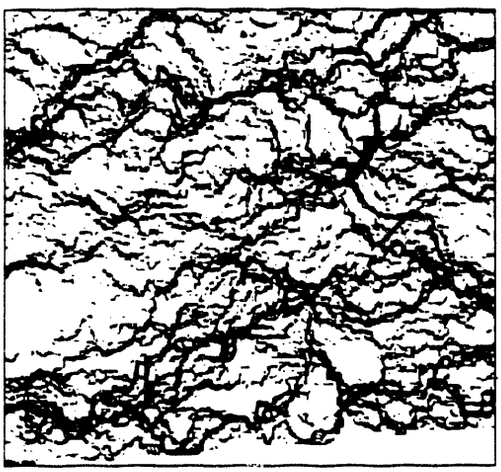

(b)

(d)

Figure 4. Representation of calculated flow fields in (a) Bandelier tuff fracture, (b) Tram tuff fracture, (c) Bullfrog tuff fracture, and (d) Bullfrog tuff fracture with flow rotated 90-degrees relative to (c). Darker shades indicate regions of higher volumetric flow rates. Flow direction in all images is from left to right with no-flow boundaries on top and bottom. Relative sizes of images are same as relative sizes of fractures. High flow regions generally correspond to regions of higher aperture. By comparing these images to Figure 4, it is apparent that dispersion is generally greater in fractures with a smaller number of flow channels.

erroneous accumulation of particles in stagnant zones noted by Tompson and Gelhar[12] when dispersivity and porosity gradients are ignored in particle-tracking calculations.

- Fracture walls are always treated as reflective boundaries for colloid particles. However, colloids are subject to hydrodynamic corrections,[13] which cause a gradient in diffusivity and an advective velocity slightly different from that of the free fluid when the particles are close to a wall. These corrections are included in the calculations.

Breakthough curves were obtained from the particle-tracking calculations by plotting the cumulative distribution of particle residence times within the flow domains. Figure 5 shows a comparison of calculated and experimental breakthrough curves for both colloids and iodide. Also shown is a calculated breakthrough curve for particles that simply experience the average fluid residence time in each cell they encounter, which is a technique commonly used in particle-tracking calculations for variable aperture fractures.[8,10] Although our calculations are considered preliminary at this time, it is apparent that they provide additional detail that at least qualitatively agrees with the observed experimental behavior of both the colloids and the iodide. We speculate that the underprediction of colloid concentrations and the overprediction of iodide concentrations shown in Figure 5 (a common feature of model predictions in all fractures) may indicate that the colloids actually experience a smaller effective volume and/or the iodide experiences a larger effective volume than what we assumed to be the void volume. This could occur if the fracture walls have fine-scale roughness that results in stagnant regions along the walls that the colloids are excluded from and the iodide has access to because of its greater diffusivity. Of course, we cannot rule out other possible explanations for discrepencies between experiment and model: (1) errors in the aperture distributions deduced from the surface profile data, (2) nonvalidity of the local parallel-plate approximation in the flow and particle tracking calculations, and (3) other invalid assumptions in the particle tracking calculations. We shall continue to investigate these possibilities. Although not shown here, our calculations also predicted the same trend of dispersion in the fractures that is shown in Figure 3.

CONCLUSIONS

We believe that we have demonstrated at the laboratory scale a novel approach for estimating how much of the observed dispersion of a nonsorbing solute in a saturated natural fracture can be attributed to matrix diffusion. This approach also allows the study of colloid transport in fractures under conditions of minimal deposition. Our modeling efforts have proven

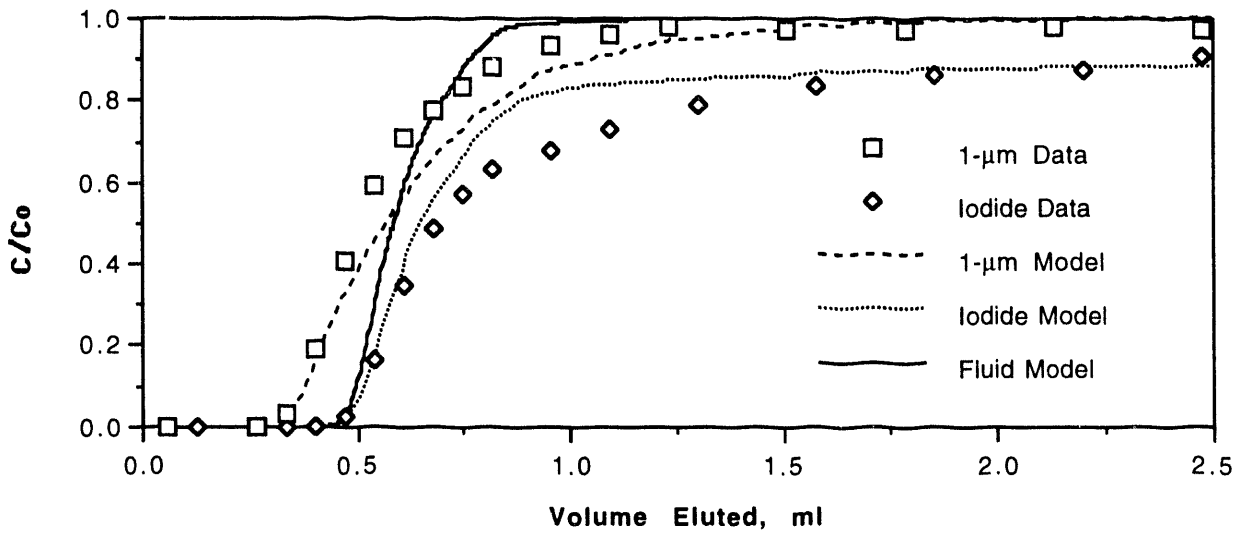

Figure 5. Comparison of experimental breakthrough curves and model results (based on 1000 particles) for the 1-µm CML colloids and iodide in the Bandelier tuff fracture at a flow rate of 2.30 µl/sec. "Fluid Model" refers to calculations in which the particles simply experienced the average fluid residence time in each cell they encounter.

successful in that many of the features of the experimental breakthrough curves of both the colloids and the iodide have been qualitatively reproduced. In the future, we plan to conduct field experiments with colloids and solutes as tracers in an attempt to apply what we have learned to larger scales.

ACKNOWLEDGMENTS

The authors wish to thank Bill Durham of Lawrence Livermore National Laboratory for the use of the PEAK profilometer to obtain three-dimensional profiles of each fracture surface. We also thank Robb Habbersett of Los Alamos National Laboratory for his assistance in determining polystryene microsphere concentrations using Los Alamos' "Big Geek" flow cytometer. Ines Triay of Los Alamos conducted a peer review of this paper.

This work was supported by the Yucca Mountain Site Characterization Project Office as part of the Civilian Radioactive Waste Management Program. This Project is managed by the U.S. Department of Energy, Yucca Mountain Site Characterization Project. In accordance with Administrative Procedure 5.1Q, this paper contains no new scientific or engineering data.

REFERENCES

1. J. F. McCarthy and J. M. Zachara, Environ. Sci. Tech., **23**(5), 496 (1989).

2. P. A. Smith and C. Degueldre, J. Contaminant Hydrology, **13**, 143 (1993).

3. I. Neretnieks, in Flow and Contaminant Transport in Fractured Rock, edited by J. Bear, C.-F. Tsang, and C. de Marsily (Academic Press, New York, 1993) pp. 56-80.

4. P. Maloszewski and A. Zuber, Water Resources Res., **29**(8), 2723 (1993).

5. P. W. Reimus, B. A. Robinson, H. E. Nuttall, and R. Kale, in Preprints of Papers Presented at the 207th ACS National Meeting, **34**(1), (American Chemical Society, Division of Environmental Chemistry, 1994) pp. 431-434.

6. W. B. Durham and B. P. Bonner, Int. J. Rock Mech. Min. Sci. & Geomech Abstr., **30**(7), 699 (1993).

7. P. W. Reimus, B. A. Robinson, and R. J. Glass, in High-Level Radioactive Waste Management, Proceedings of the 4th Annual International Conference, (American Nuclear Society, LaGrange Park, Illinois) pp. 2009-2016.

8. C.-F. Tsang, in Flow and Contaminant Transport in Fractured Rock, edited by J. Bear, C.-F. Tsang, and C. de Marsily (Academic Press, New York, 1993) pp. 242-250.

9. D. W. Peaceman and H. H. Rachford, Jr., J. Soc. Indust. Appl. Math., **3**, 28 (1955).

10. L. Moreno, Y. W. Tsang, C. F. Tsang, F. V. Hale, and I. Neretnieks, Water Resouces Res., **24**(12), 2033 (1988).

11. P. W. Reimus, Fh.D. Thesis, University of New Mexico (in preparation).

12. A. F. B. Tompson and L. W. Gelhar, Water Resources Res., **26**(10), 2541 (1990).

13. T. G. M. Van de Ven, Colloidal Hydrodynamics (Academic Press, New York, 1989).

DATE
FILMED
11/17/94

END